Journal of Mining and Earth Sciences

Website: http://jmes.humg.edu.vn

Rainfall-Runoff and Inundation of Ma River Basin Under Global Warming

Quan Anh Tran [1*], Ngoc Hong Thi Nguyen [2], Huong Thu Thi Tran [1], Hai Thi Do [1], Ha Kim Thi Tran [1]

[1] *Hanoi University of Mining and Geology, Vietnam*
[2] *Vietnam National University of Agriculture, Vietnam*

ARTICLE INFO

Article history:
Received 15th Aug. 2019
Accepted 16th Oct. 2019
Available online 30th Dec. 2019

Keywords:
Climate change,
Inundation,
Ma,
RRI,
Vietnam.

ABSTRACT

Vietnam has been considered as one of the most vulnerable countries in the world under global warming. The Intergovernmental Panel on Climate Change (IPCC) estimated the increasing trend in the total annual rainfall in Vietnam in the mid-21st century, where 70% of the amount of rainfall will be delivered by the summer monsoon. The most problematic rainfall-related disasters in the northern mountainous regions in Vietnam, floods and inundations, are also expected to become even more severe in the coming future. In recent years, the Ma river basin has been undergoing the noticeably increasing trend of flood disasters. Since Ma River basin plays an important role in the development of the vast Lai Chau - Son La - Thanh Hoa economic regions, establishing the solid understanding of the current and future hydro-meteorological characteristics of the Ma watershed is very important to prepare the countermeasure for the coming severe variation in rainfall intensity and frequency. In this research, the rainfall-runoff and inundation characteristics of the Ma watershed have been investigated associated with the corresponded climate conditions of the present (2000-2009) and future (2060-2069). The Rainfall-Runoff and Inundation (RRI) model were used for the simulation of watershed hydrological characteristics. The essential future precipitation inputs for RRI were achieved by using the Weather Research and Forecasting (WRF) model nested inside GFDL-CM3, and MIROC-5 models. The results of this study suggest the severe flood and inundation condition of Ma watershed in the mid-21st century.

**Corresponding author*
E-mail: quantrananh.humg@gmail.com

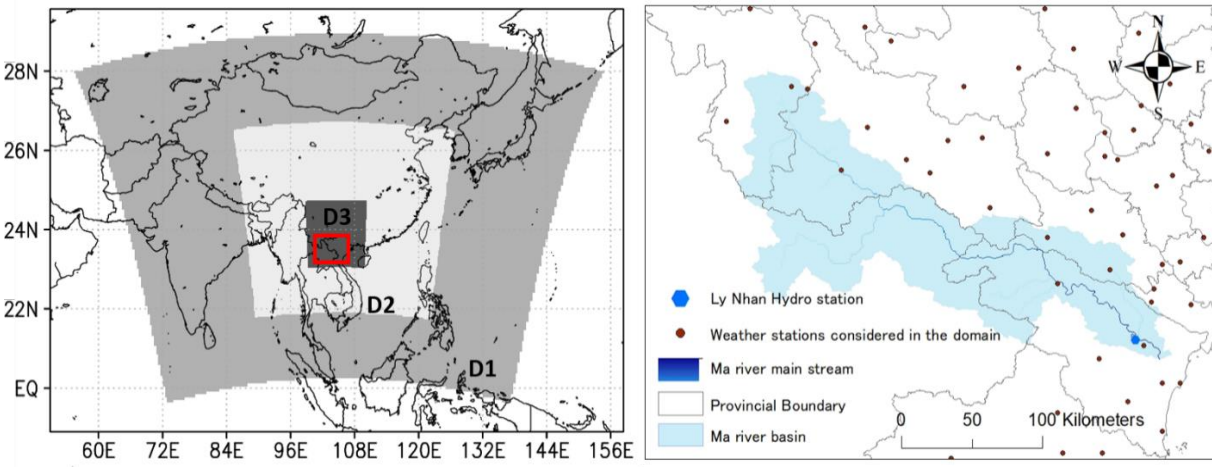

Figure 1. The target areas for WRF models, in which (a) The outermost 90 km resolution (D1), the middle 30 km resolution domains (D2) and the innermost 10 km resolution are shown in the grey, white, and dark grey colors, respectively, the red rectangular indicate the locations of the researching area; (b) Locations of Ma watershed and hydro-meteorological station.

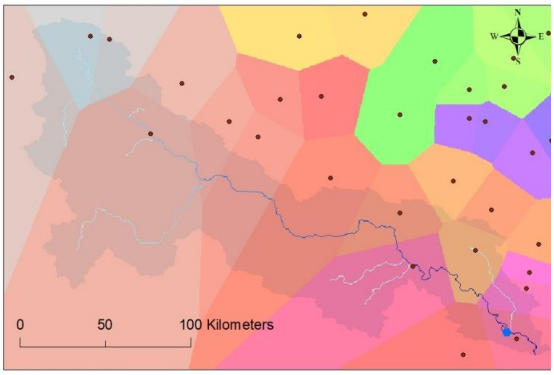

Figure 2. Coverage of weather stations considered in this study as the results of inverse distance interpolation.

1. Introduction

The Intergovernmental Panel on Climate Change (IPCC) has forecasted the increasing trend of global surface temperature by 1÷2°C at the end of 2050 and might rise to 2÷5°C at the end of the century (IPCC, 2013). Global warming over the past several decades was accounted for various natural disasters throughout the world. In the recent publication IPCC's Fifth Assessment Report (AR5), climate change was proven the culprit behind the damages caused by harmful disasters in many regions, Southeast Asia (SEA) is known as one of those heavily vulnerable regions. Located in SEA, Vietnam has been considered one of the most affected countries in the world under climate change. Vietnam's northern mountainous region is the poorest region of the country but highly susceptible to flood and inundation during the rainy season. Flood and inundation are the most destructive natural disasters that happened every year and resulted in the great economic and social loss. Experts have forecasted the growing risks of these hazards in northern Vietnam in the mid-21 century and indicated the need of better awareness as well as the more effective flood risk prevention and management (Quan and Taniguchi, 2018).

Future changes in rainfall intensity account for the variations in flood runoff. This study focuses on the flooding and inundation problems for one of the most important river basins in northern Vietnam. Figure 1(a) shows the researching area with the location of Ma watershed placed in the center of the domain. This is one of the major rivers running through the territory of five provinces. The Ma river basin plays an important role for the development of the region as it provides domestic and production water sources for the vast populated-economic regions. Ma watershed was formed in the high mountain range in the Dien Bien province then flows southward with the lower river basin placing on the flat plateau. Three domain nesting setups are expected to increase the accuracy of weather simulation as the separation of the boundary layer will be provided with more resolution.

The number of flood occurrence in Ma watershed has rapidly increased recently. In the theme of global warming, it is important to prepare the countermeasures and mitigation methods to cope with the potential risks. It is impossible to establish action plans without a deep understanding of the characteristics of the flood in accordance with the present and future hydro-meteorological conditions. The traditional simulation method for inundation researches combines both rain-fall-runoff models for river discharge and hydraulic model for water propagation. However, this method is not suitable for flat watershed with large inundation areas as it requires significant calculations between the river and floodwater. This study, therefore, uses the Rainfall-Runoff Inundation (RRI) model, which is a fully coupled model of the rainfall-runoff model and hydraulic inundation model (Sayama et al., 2012). Besides, the Weather Research and Forecast (WRF) model (Skamarock et al., 2009) was also employed to provide present and future input precipitation for the RRI model.

2. Research data and materials

2.1. In-situ daily observation data

The in-situ rainfall data collected by the Vietnam National Centre for Hydro-Meteorological Forecasting (NCHMF) at 56 rain gauges station from 2000÷2009 provides a basis for this study. Selected stations are similar in monitoring techniques without missing value. However, since the locations of those rain gauges are scattered around the whole northern region so after analyzing the coverage of each and every rain gauges by inverse distance interpolation method, the total number of weather stations contributed to the hydrological simulation are 15 out of 56. Details of the coverage region by weather stations are illustrated in Figure 2.

As river discharge data for verification of RRI simulation results, we used monitored data in July and August 2009 from Ly Nhan hydraulic stations which locate in a major branch of Ma river system. Locations of hydro-meteorological stations are shown in Figure 1(b). Northern Vietnam climate is distinguished by the Southeast Asia monsoon system with the hot-rainy season from Jun to August (JJA) then the cold-dry season from December to February (DJF). In this study, we focused on the hydro-meteorological condition of the Ma river system during the JJA period.

2.2. Global Satellite Mapping of Precipitation (GSMaP)

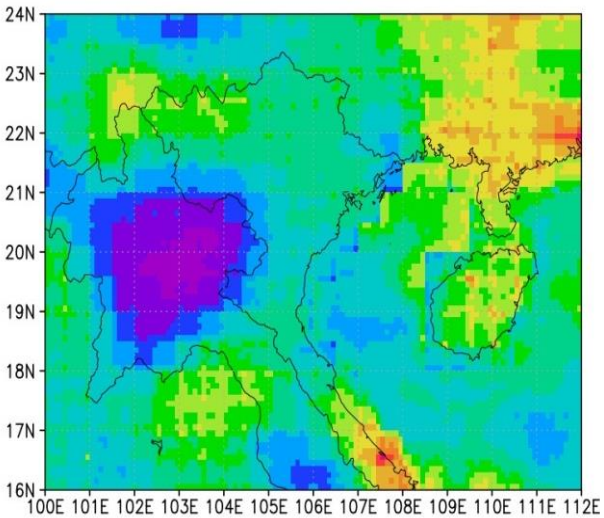

Figure 3. GSMaP dataset for northern Vietnam.

Since one-third of the Ma river basin position outside Vietnam territory belongs to the administrative region of Laos, in Lao, the Ma river basin is called the Nam Ma river. However, it is very difficult to obtain the observation climatology condition of the Nam Ma river as those data belong to the Laos government. Such missing data over one-third of the domain exhibited the lack of the accuracy and reliability of hydraulic simulation. To overcome the shortage of data and to fill the missing value, here in this study, we use the Global Satellite Mapping of Precipitation (GSMaP) dataset. GSMaP is the product promoted for a study "Production of a high-precision, high-resolution global precipitation map using satellite data," sponsored by Core Research for Evolutional Science and Technology (CREST) of the Japan Science and Technology Agency (JST) during 2002-2007. This dataset has been known as one of the most reliable alternative rainfall data for the global scale. For the verification of the past climate events, GSMaP data has been extracted for the year 2009 (Figure 3).

2.3. CMIP5 global warming experiments

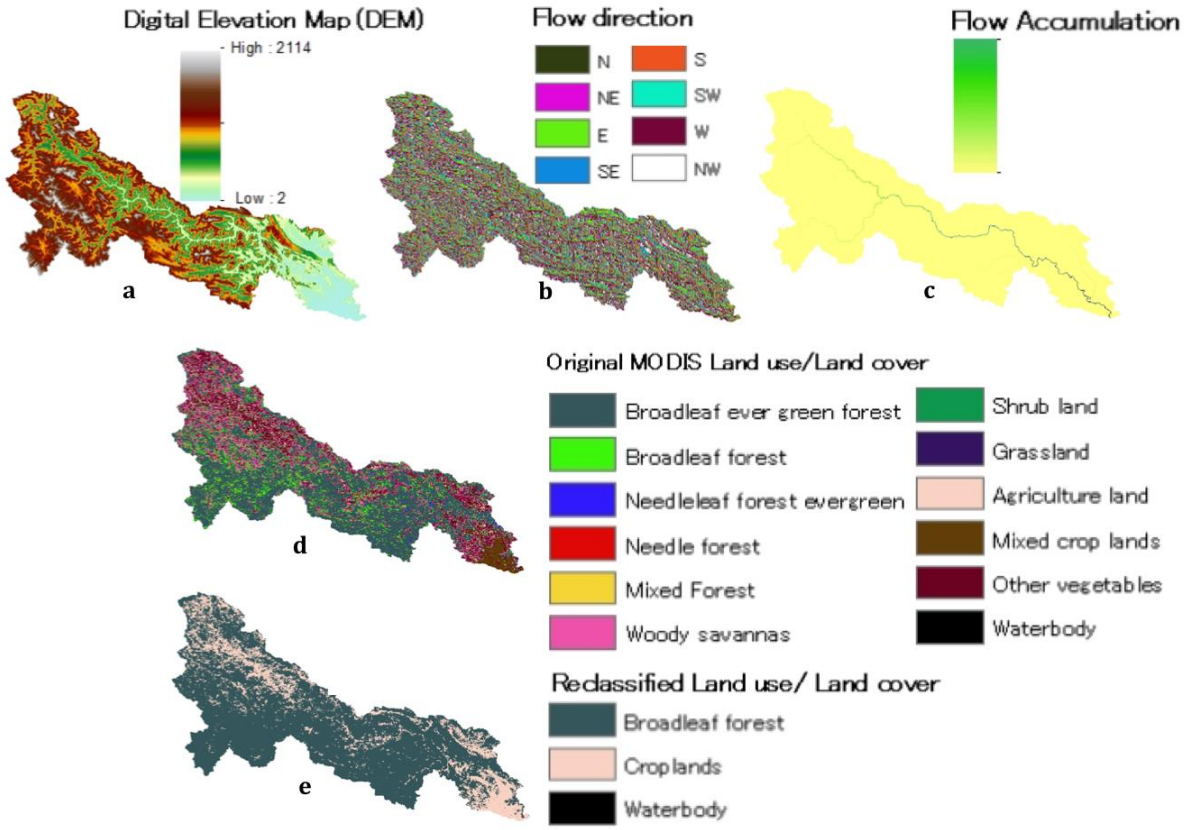

Figure 4. Topography and land use inputs for RRI model.

For assessment of future global warming, this study based on the global warming experiments by the fifth phase of the Coupled Model Inter-comparison Project (CMIP5). Numerous experiments provided by CMIP5 represent the state-of-the-art international assessment of climate science. The future climate projections in CMIP5 are based on different future greenhouse emission scenarios known as representative concentration pathways (RCPs). Herein, we examined the daily precipitation for the mid-21st century from 2060 to 2069. In Vietnam, the progress of climate change is taking place faster than expected. Recently, the Vietnam government has updated the high emission scenario RCP8.5 in the national strategy on climate change to propose the action plan for extreme weather events under the worst-case scenario (MONRE, 2012). In RCP8.5, the radiative forcing of the Earth become 8.5 W/m^2 larger than before the industrial revolution. In this study, we used the output of two Atmosphere-Ocean General Circulation Model (AOGCM) projections from NOAA Geophysical Fluid Dynamics Laboratory Climate Model version 3 (GFDL-CM3) (Griffies et al., 2011) and a new version of Model for Interdisciplinary Research on Climate (MIROC-5) (Wanatabe et al., 2010) for preparation of the future conditions.

2.4. Initial and boundary conditions for numerical weather simulation

This study uses a Japanese 25-year reanalysis (JRA-25) produced by The Japan Meteorological Agency (JMA) for reproducing the present climate conditions, which are also the base state for the future (pseudo global warming) conditions. The global spectral resolution of JRA-25 is kept at T106 with 40 vertical layers where 0.4 hPa was set for the height of the top level. Since the JRA-25 only provides the assimilation data from January 1979 to December 2004, the

reanalysis product from the JMA Climate Data Assimilation System (JCDAS) has been used for the period from January 2005. JCDAS deploys a similar system as JRA-25, which guarantees the homogeneous in quality and accuracy in the application of both datasets. The current climate conditions were obtained by performing dynamical downscaling to the 2000÷2009 data. Simulation results for climate conditions (or control simulation) are called CTL.

For land-surface boundary conditions for the WRF model, we used the NCEP Final Operational Global Analysis data (NCEP FNL)(NCEP, 2014). For the lower boundary condition over the ocean, the NOAA Optimum Interpolation 1/4 Degree Daily Sea Surface Temperature Analysis (NOAA OI SST) was used (Reynolds et al., 2007).

2.5. Topography and global land cover data

Input data for the RRI model was taken from the hydrological data and maps based on Shuttle Elevation Derivatives at multiple Scales (HydroSHEDS). Topography inputs of 15-arc second resolution (approximately 500m) for the digital elevation model, flow accumulation, and flow direction were used for the RRI model (Figure 4(a,b,c)). Regarding the RRI requirements of land cover data, we used the Moderate Resolution Imaging Spectroradiometer (MODIS) based product of 0.5 km resolution (Figure 4(d,e)). The original MODIS dataset over the Ma river basin composed of 12 land-use types was reclassified into 3 types to simplification of the simulation setting as detailed information for the characteristics of each, and every soil type is not available.

3. Methodology

3.1. Design of numerical simulation

3.1.1. The Weather Research and Forecasting model

Downscaling of present and future climate conditions was implemented using the WRF model version 3.6. A two-level, two-way nesting system for WRF downscaling is shown in Figure 1(a), where D1 and D2 represented for the 30km and 10km grid spacing resolution, respectively. The Ma watershed locates in Northern Vietnam where placed in the center of the D2 domain. The WRF Double-Moment 5-class scheme (WDM5) microphysics and Grell-Devenyi cumulus parameterization schemes were used to calculate precipitation in the model. Planetary boundary layer parameterization is used from the Mellor-Yamada Nakanishi and Niino Level 2.5 PBL (MYNN2). The used parameterization for the surface layer and land surface are taken from Nakanishi and Niino PBL's surface layer scheme and Noah land surface model, respectively. The new Rapid Radiative Transfer Model (RRTMG) schemes are selected for longwave radiation and shortwave radiation conditions.

3.1.2 High-frequency-anomaly PGW

Downscaling simulations for present and future climate conditions were prepared with pseudo global warming force. The lateral boundary conditions for the future were constructed by adding projected changes in AOGCM simulations to reanalysis climate. In this study, the high-frequency anomaly pseudo global warming (HF-PGW) methods were applied to prepare the initial forcing with future high-frequency anomalies (Taniguchi, 2016). The future inter-annual variability and the diurnal cycle can differ from the present climate. At first, six-hourly AOGCM and reanalysis dataset (RD) were divided into climatological monthly mean plus the short perturbation terms:

$$AOGCM_P = \overline{AOGCM}_P + AOGCM'_P \quad (1)$$

$$AOGCM_F = \overline{AOGCM}_F + AOGCM'_F \quad (2)$$

$$RD_P = \overline{RD}_P + RD'_P \quad (3)$$

The subscript *P* and *F* represent the present (2000-2009) and the future (2060-2069), respectively. Then the bias-corrected six-hourly AOGCM data for the future period, $AOGCM*_F$, was calculated by adding the climatology variation between future and present ($\overline{AOGCM}_F - \overline{AOGCM}_P$) and short term perturbation $\overline{AOGCM}_F'$ to climatological mean reanalysis: $AOGCM*_F = \overline{RD}_P + \overline{AOGCM}_F - \overline{AOGCM}_P + AOGCM'_F$ (4)

The inter-annual variation and diurnal circle were both included in HF-PGW conditions, which are expected to greatly reduce the bias in AOGCM outputs.

3.2. RRI model

RRI model has been used to simultaneously simulate the conditions of

rainfall-runoff and flood inundation for the research domain (IPCC, 2013). In the RRI model, both slope and river are assumed within the same grid cell. The river channel is considered as a single line on the overlying slope cells. The 2-dimension diffusive wave model was adopted to calculate the flow over slope grid cells, while the 1-dimension diffusive wave model was applied for the main channel flow. For better representation, the rainfall-runoff-inundation processes of Ma watershed, the surface/subsurface condition parameterization was enabled with vertical Green-Ampt model infiltration flow. Since the original MODIS product includes 16 types of land use, which is too detailed to designate all the parameters, similar land cover types were combined into four major categories and also overlaid with the river floodplain region (Figure 4(e)). Human management activities to control and regulate the river channel were considered with a dam model. The evaporation parameter in the RRI model was disabled due to the lack of detailed monitored evaporation data. The simulation result of RRI for 2009 was used for model verification.

4. Simulation results of historical flood inundation

In this section, we verify the accuracy of rainfall downscaling by WRF from 2000÷2009 by using the observation data (OBS) from 56 rain gauges. The RRI simulation results have also been examined for the 2009 flood event at Ly Nhan hydro station.

4.1. Reproducibility of the WRF model

Figure 5 compares the JJA rainfall averaged for 56 rain gauges and corresponding CTL grids from 2002 to 2009. It can be seen from the results that JJA rainfall reproduced by CTL varied from 73.5% to 92.2% of observation data and consistently underestimated. The average spatial correlation coefficient for 10 years (2000-2009) calculated between CTL and OBS was 0.77, indicates the relatively good agreement between simulation results and observation. Regarding the temporal variation of rainfall, correlation coefficients between CTL and OBS averaged for

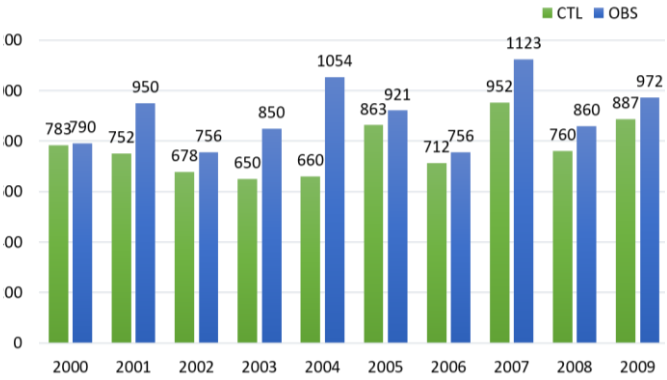

Figure 5. JJA rainfall averaged for 56 observation sites and corresponding grids in CTL from 2000 to 2009.

JJA periods in 10 years in 56 observation sites range from 0.52 to 0.89 with an average of 0.7 (details not shown). The verification result indicates the WRF model can be used for rainfall downscaling in Ma watershed with reasonable accuracy.

4.2. Simulation of RRI models for historical flood events

Observation rainfall data in July-August 2009 was fed into the RRI model to examine the accuracy of the model to represent the flood events. The missing data at mid-stream, which belongs to Laos territory, is replaced with GSMaP data of 0.25 degree resolution. A comparison of river discharge between RRI simulated results (RRI-CTL) and observation data was shown in Figure 6. The Nash-Sutcliffe efficiency coefficient (NSE) was used to quantitatively describe the predictive power of RRI model outputs for river discharge. NSE indexes calculated at Ly Nhan stations are relatively high with 0.64. NSE results showed a good match between simulated results and OBS in the decreasing trend of river discharge at the end of the rainy season. Since the NSE index insensitive to extreme value, the high NSE results also suggested that extreme discharge periods were relatively well predicted. Simulation results slightly overestimated the peaks of river discharge in Ly Nhan station. However, the peaks of large and small floods are correctly reproduced in RRI simulation. Verification results show the good applicability of adopting

the RRI model to further investigate the future hydrological condition of the Ma river system.

5. Future flood forecasting

5.1. Future trend in rainfall intensity

WRF daily rainfall outputs during JJA for 10-years periods of CTL (2000-2009), GFDL-CM3, and MIROC-5 (2060÷2069) were used as inputs for RRI model to examine the variation of rainfall distribution over the Ma river basin. Spatial distribution of 10-years average JJA rainfall clearly shows the future higher intensity of rainfall throughout the watershed (Figure 7). Average JJA rainfall indicated by CTL, MIROC-5, and GFDL-CM3 were 781 mm, 928 mm, and 981 mm, respectively. While GFDL-CM3 predicted small rainfall variation (20.1% increment), there was a significant gap between MIROC5 and CTL (30.2% increment). Rainfall forecasted by MIROC5 was 6% greater than GFDL-CM3. Thanh and Taniguchi (2013) used 19 CMIP5 models ensemble and found the same increasing trend of rainfall over northern Vietnam in the second half of the 21st century. The same results were also found by experts of MONRE (Thuc et al., 2017). Future scenario forecasted by both GFDL-CM3 and MIROC-5 indicated the similar rainfall distribution patterns with the present where the major amount of JJA rainfall concentrated on the upper river basin, especially the far north and eastern corner. The featured distribution of

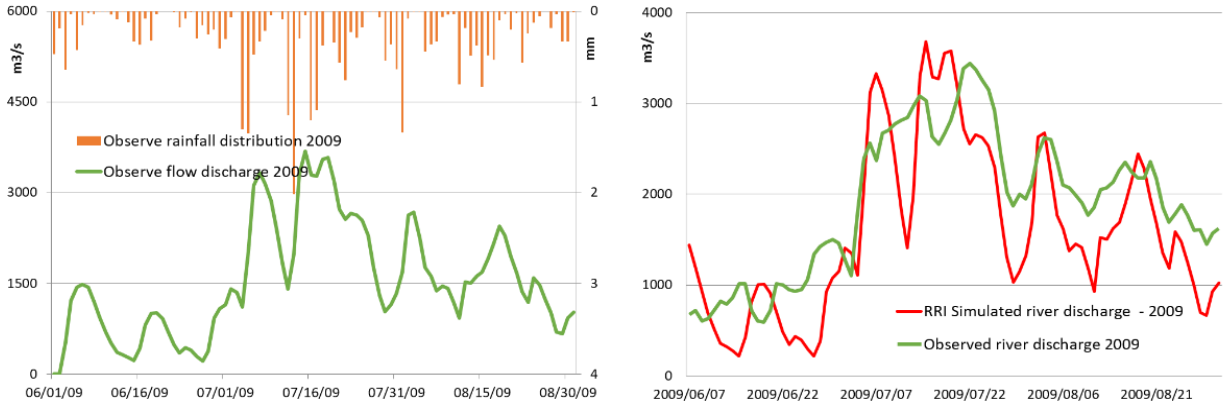

Figure 6. Basin mean precipitation and river discharge by RRI model and observation data in Ly Nhan stations during JJA in 2009.

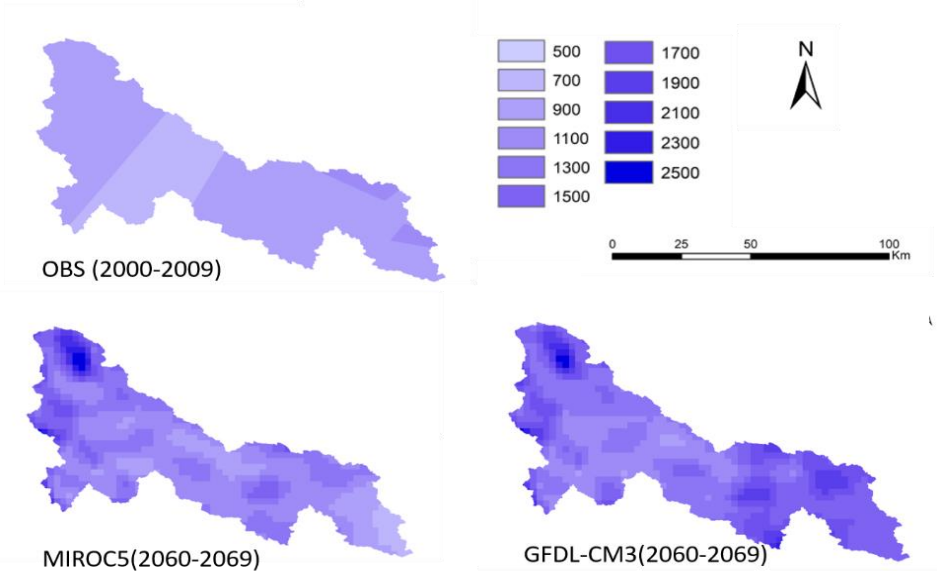

Figure 7. Spatial distribution of 10-years average JJA rainfall.

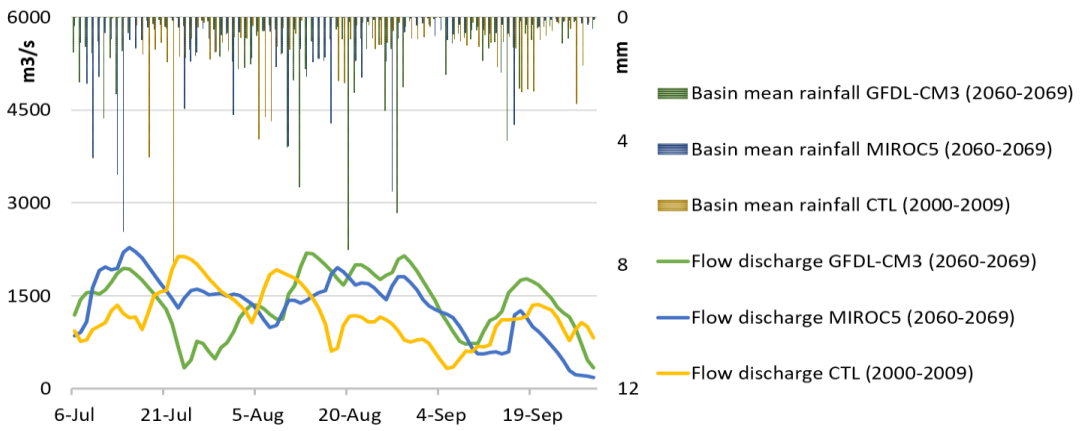

Figure 8. Daily precipitation and river discharge for present and future condition at Ly Nhan stations.

rainfall patterns in Ma watershed results from its typical topographic conditions.

5.2. Future trend of flood and river runoff

Future precipitation was predicted to increase during the mid-21st century. Increasing river discharge found in Figure 8. RRI simulating river runoff in CTL (2000-2009) was comparable with GFDL-CM3 and MIROC-5 (2060÷2069) in the middle period of the rainy season with no significant difference in average river discharge. Differences caused by higher rainfall intensity in the future scenario was found mostly in the latter half of the rainy season when future river discharge was projected larger than CTL. In the late JJA period, GFDL-CM3 model showed average river discharge will significantly increase, almost double as in CTL in Ly Nhan station. Meanwhile, MIROC-5 exhibited lower average river discharge than GFDL-CM3 as expected while future precipitation in GFDL-CM3 is projected much higher than in MIROC-5. Future river discharge in MIROC-5 is slightly larger than in CTL at during the peak runoff period and equal to CTL at the end of rainy season. In Ly Nhan station which locates in the largest branch of Ma watershed, MIROC-5 shows clear higher average discharge than in CTL. After JJA ends, river discharge tends to reduce in both three cases. While MIROC5 and GFDL-CM3 forecast the future river discharge after the rainy season significantly reduced, CTL indicates that discharge had not changed much.

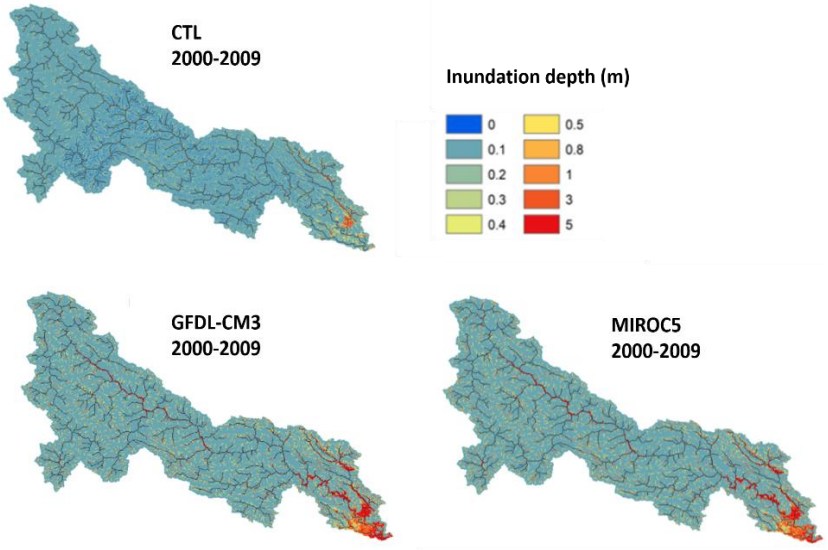

Figure 9. Maximum level of inundation depth in Ma watershed during JJA.

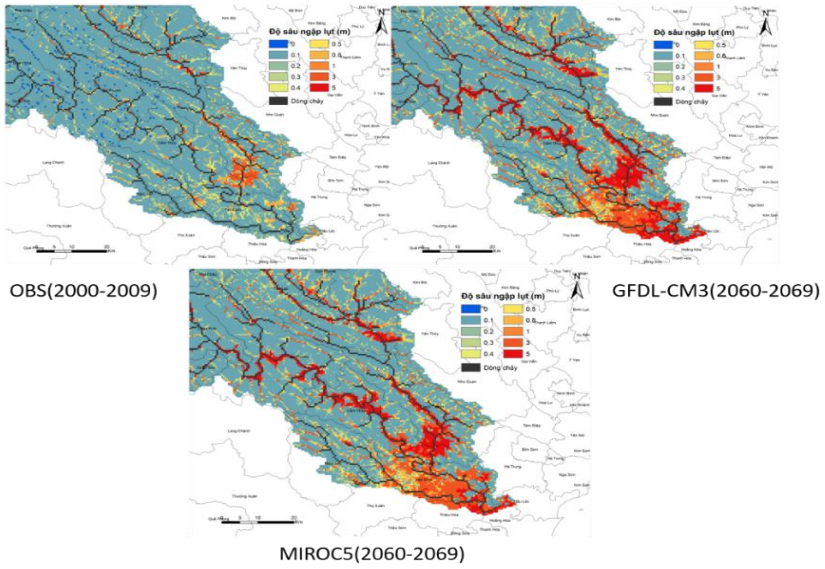

Figure 10. Inundation depth and lower Ma river basin.

Figure 9 illustrates the maximum inundation depth by CTL and future projections over the whole river domain. Since the topography of the Ma river is characterized by the high elevation in the upper basin the gradually lower toward the flow direction, the lower basin captures only a small area of the lower river basin where locates the most important socio-economic objects of the region. Inundation due to heavy rainfall and extreme events, therefore, is projected to occur only in the lower part of the river basin. In most part of the Ma river is safe from severe flooding except for the areas close to the mainstream.

Figure 10 illustrates the detailed projections for the lower river basin compared with the simulation results of the CTL period. The distribution map for maximum depth was prepared by selecting the highest value of depth for every grid in the Ma watershed during a 10-year period. Variation of maximum inundation depth represents the changes in the worse situation which might happen. Both GFDL-CM3 and MIROC-5 show the huge difference in maximum inundation level from in CTL. The worst CTL situation indicates the inundation level of about 0.5 to 1.5 meters depth at the areas far from the river channel; closer to the river channel, the influence level becomes greater of 1.5 to 3 meters depth and up to 5 meters at some few locations (excluding river channel). Projection by GFDL-CM3 and MIROC-5 both indicate the more severe inundation in the lower river basin, about 1.5-2 meters higher than in CTL. Extreme flood (inundation depth > 3 meters) occurs in more locations with extended inundation radius. Closer to main river channels at the downstream, the common inundation depth caused by the worst future flood situation in GFDL-CM3 and MIROC-5 are 2-3 meters, much higher than CTL. Comparing GFDL-CM3 to MIROC-5, the worst inundation situation in GFDL-CM3 was more intense for the most locations. Increase in the mean JJA rainfall and river discharge is larger in GFDL-CM3 than in MIROC-5. However, the maximum inundation depth is larger in MIROC-5. These results suggest that the amplitude of climate variability in MIROC-5 is stronger than in GFDL-CM3. Since the comparison between CTL and future river runoff only exhibits clear differences between late July/early August, it is projected that the severe future flood conditions tend to occur in the late JJA period.

6. Conclusion

In this study, the present and future rain-fall-runoff and inundation conditions of the Ma river basin during JJA were examined using the combination of WRF and RRI models. While simulation results of WRF for the present precipitation showed reasonable accuracy for temporal and spatial distribution, reproductive

RRI results for Ma river discharge came relatively close to OBS. Generally, both WRF and RRI models are capable of deploying further assessment on the future river basin conditions.

The future downscaling results by GFDM-CM3 and MIROC-5, indicated heavier rainfall conditions in the mid-21st century and consequently cause more severe inundation conditions. At the first half of JJA, there is no significant difference in average river runoff conditions between CTL and future projections, heavy rainfall and inundation were expected to increase in the second half of JJA. In both GFDL-CM3 and MIROC-5, the impacted areas due to flood will increase in both spatial and temporal extent, intensity, and density. MIROC-5 model forecasted the extreme flood might occur in late JJA. Future inundation conditions will affect mostly the agricultural and residential areas in the lower Ma river basin. This study suggests further assessments on the impacts of the future flood to agriculture and the environment as well as the needs of studies on an adaptive management plan.

Acknowledgments

The authors would like to thank the Vietnam National Centre for Hydro-Meteorological Forecasting (NCHMF), the Japan Meteorological Agency (JMA), the Conservation Science Program of World Wildlife Fund (WWF) and U.S. Geological Survey (USGS) for their help in researching the data. We would be grateful for the anonymous reviewers for their suggestions.

References

Griffies, S.M., et al., 2011. The GFDL CM3 Coupled Climate Model: Characteristics of the Ocean and Sea Ice Simulations. *Journal of Climate*. 24(13): p. 3520-3544.

IPCC, Climate Change 2013: The Physical Science Basis. Contribution of Working Group I to the Fifth Assessment Report of the Intergovernmental Panel on Climate Change. Cambridge, United Kingdom and New York, NY, USA: *Cambridge University Press*. 1535, 2013.

MONRE, 2012. Climate change, sea-level rise scenarios for Vietnam. *Ministry of Natural Resources and Environment*. Vietnam.

National Centers for Environmental Prediction/National Weather Service/NOAA/U.S. Department of Commerce, 2000. *NCEP FNL Operational Model Global Tropospheric Analyses, Continuing from July 1999*. Accessed 12. June. 2014 http://dx.doi.org/10.5065/D6M043C6.

Reynolds, R.W., Smith, T.M., Liu, C., Chelton, D.B., Casey, K.S., Schlax, M.G., 2007. Daily high-resolution-blended analyses for sea surface temperature. *J. Clim*. 20 (22), 5473–5496, http://dx.doi.org/10.1175/2007JCLI1824.1.

Sayama, T, 2012. Rainfall–runoff–inundation analysis of the 2010 Pakistan flood in the Kabul River basin. *Hydrological Sciences Journal*. 57(2): p. 298-312.

Skamarock, W.C., Klemp, J.B., Dudhia, J., Gill, D.O., Barker, D.M., Huang, X.Y., and W. Wang, Powers, J.G, 2009. A Description of the Advanced Research WRF Version 3. *Technical Note*. NCAR/TN-475 + STR.

Taniguchi, K., 2016. Future changes in precipitation and water resources for Kanto Region in Japan after application of pseudo global warming method and dynamical downscaling. *Journal of Hydrology: Regional Studies*. 8: p. 287-303.

Thuc, T, et al., 2017. Estimating Sea Level Rise for Vietnam East Sea. *Environmental Science: Climatology.* 1(1):p. 73-77.

Tran Anh, Q. and K. Taniguchi, 2018. Rainfall runoff and inundation in Cau-Thuong-Luc Nam watershed in Vietnam under global warming, *Journal of Japan Society of Civil Engineers, Ser. B1 (Hydraulic Engineering), Vol. 74, No. 4, pp.I_163-168, 2018, 04.*

Tran Anh, Q. and K. Taniguchi, 2014. Variations of precipitation and water resources in the Northern part of Vietnam under climate change. *Journal of Japan Society of Civil Engineers, Ser. B1 (Hydraulic Engineering)*. 70(4): p. I_211-I_216.

Watanabe, M, 2010. Improved Climate Simulation by MIROC5: Mean States, Variability, and Climate Sensitivity. *Journal of Climate*. 23(23): p. 6312-6335.